Enhancing Interlayer Bonding in GF/PEEK Additive Manufacturing via Optimized Heat Input

LI Haozhen, XIAO Xingzhi, LIAO Wenhe*, LIU Tingting*

College of Mechanical Engineering, Nanjing University of Science and Technology, Nanjing 210094, P. R. China

(Received 27 May 2025; revised 29 September 2025; accepted 10 December 2025)

Abstract: To address the insufficient interlayer mechanical properties of glass fiber-reinforced polyetheretherketone (GF/PEEK) composites fabricated by fused deposition modeling (FDM), resulting from the impracticality of post-process heat treatment for large-scale components and structural circuit-integrated components, an in situ thermal radiation-assisted strengthening method was proposed to enhance the interlayer mechanical properties along the build direction. The mechanical properties and interlayer strengthening mechanism of GF/PEEK composites under different thermal treatment strategies were systematically investigated by regulating the chamber temperature and in situ thermal radiation power, combined with tensile tests, interlayer tensile tests, and fracture surface morphology analysis. The results showed that increasing the chamber temperature improved the tensile properties in the horizontal direction. At a chamber temperature of 200 ℃, the tensile strength and Young's modulus reached 62.72 MPa and 3.45 GPa, respectively. However, the interlayer tensile strength decreased from 20.61 MPa to 6.03 MPa, while the interlayer Young's modulus increased from 1.90 GPa to 2.24 GPa. By contrast, in situ thermal radiation significantly enhanced the interlayer mechanical properties of specimens fabricated along the build direction. At a thermal radiation power of 255 W, the vertical tensile strength and fracture elongation increased to 2.34 and 7.91 times those of conventional FDM specimens, respectively, achieving mechanical properties comparable to those of post-process heat-treated specimens. Fracture surface analysis further revealed that in situ thermal radiation promoted interlayer polymer chain diffusion and molecular entanglement while reducing interfacial defects, thereby substantially improving the interlayer bonding performance. The proposed method effectively enhances the interlayer mechanical properties of FDM-fabricated GF/PEEK composites without requiring an additional post-process heat treatment, providing an effective processing strategy for the additive manufacturing of high-performance thermoplastic composite structures.

Key words: polyetheretherketone (PEEK); additive manufacturing; interlayer bonding strength; composite material; thermal radiation

CLC number: TB332 **Document code:** A **Article ID:** 1005-1120(2026)03-0356-15

0 Introduction

Fused deposition modeling(FDM) or fused filament fabrication(FFF) is a low-cost, high-efficiency, and versatile additive manufacturing process that constructs three-dimensional solids by heating and melting thermoplastic filaments, which are then extruded from a nozzle in layers[1-3]. Polyetheretherketone(PEEK) is a high-performance, semi-crystalline thermoplastic material known for its high strength, temperature resistance, and chemical resistance. Incorporating short glass fibers, short carbon fibers, and other reinforcing phases into the matrix to create composite materials can enhance strength, stiffness, and dimensional stability[4]. These features position PEEK composite as a promising candidate for aerospace applications[5-7]. For instance, in micro-nano-satellites and aircraft skins,

*Corresponding authors, E-mail addresses: xingzhi.xiao@njust.edu.cn; cnwho@nuaa.edu.cn.

How to cite this article: LI Haozhen, XIAO Xingzhi, LIAO Wenhe, et al. Enhancing interlayer bonding in GF/PEEK additive manufacturing via optimized heat input[J]. Transactions of Nanjing University of Aeronautics and Astronautics, 2026, 43(3): 356-370.

http://dx.doi.org/10.16356/j.1005-1120.2026.03.003

using PEEK-based composite materials as a structural substrate to manufacture conformal antennas or directly through multi-material composite moulding to achieve integrated manufacturing[8] of aircraft structural circuits will help to further realise the intelligentisation and miniaturization of equipment.

However, one of the main problems faced by the FDM process for moulding PEEK-based composites is the poor mechanical properties, especially the anisotropy of the mechanical properties of the moulded parts, i.e., the strength of the moulded parts in the horizontal moulding plane (X-Y plane) is significantly higher than that in the vertical direction (Z-direction)[9-11], and the lack of such Z-axis mechanical properties is mainly due to the low adhesion strength of the layers, which leads to the low strength and stiffness of the parts when they are subjected to the stress, which makes the parts susceptible to interlayer separation or cracking when subjected to Z-direction loading, as evidenced by many studies on the mechanical properties of PEEK and its composites. The current study shows that the factors that influence interlayer bonding are mainly two aspects: The thermal history of the moulded part and the internal pore defects of the moulded part. During the printing process of the moulded part, the cooling rate at the interfacial locations of the different deposited layers, the temperature gradient, and the time the material stays above the glass transition temperature (T_g) and melting point (T_m) have an effect on the diffusion, entanglement and crystallisation of the polymer chains, which is ultimately reflected as a change in the interlayer bonding properties[12-13]. The PEEK composite, as a semi-crystalline polymer, has crystallised regions in the interlayers that can hinder the molecular chain diffusion and movement, and the interlayer bonding situation is thus worsened. In addition, the high extrusion temperature, high melt viscosity, and poor fluidity of PEEK composites can lead to incomplete fusion of the interlayer, resulting in pore defects[14], which not only reduce the interlayer bonding area but also produce stress concentration. This also weakens the interlayer bonding properties[15].

The process parameters of molding directly affect the thermal history and internal morphology of the molded parts. Therefore, regulating the process parameters to enhance the interlayer bonding of PEEK components and reduce anisotropy is a primary research direction[16]. The extrusion temperature directly influences the material's temperature as it exits the nozzle. The higher the temperature, the stronger the polymer molecular activity, which can promote interlayer diffusion behavior and help improve interlayer bonding strength[17-18]. Curmi et al.[19] studied the interlayer shear strength (ISS) of PEEK materials at different extrusion temperatures. The experimental results showed that as the extrusion temperature increased from 380 ℃ to 400 ℃ and then to 420 ℃, the interlayer shear strength also gradually increased, reaching a maximum value of 17.70 MPa at 420 ℃. Zhou et al.[20] also proved that increasing the extrusion temperature could elevate the storage modulus and shear strength of the PEEK molded parts. However, the extrusion temperature can only be increased within a certain range due to the material's thermal degradation temperature; otherwise, it may lead to the deterioration of polymer performance. Abbas et al.[21] conducted compression tests on PEEK samples formed with different layer height parameters and found that reducing the layer height could decrease internal pores and enhance interlayer bonding, improving the compressive performance in the Z-direction. A higher thermal bed temperature or forming chamber temperature can slow down the cooling rate of the deposited layer, thereby prolonging the time required for interlayer molecular diffusion and also helping to reduce residual stress and improve interlayer bonding[20-22]. Yang et al.[23] investigated the effects of nozzle temperature, printing speed, and layer thickness on the bending performance of carbon fiber/PEEK (CF/PEEK) material under conditions without chamber and substrate heating. They found that layer thickness was the main factor affecting the performance, and the maximum bending strength obtained at a layer thickness of 0.2 mm was 50.85 MPa.

Post-heat treatment is considered an effective method to improve the mechanical properties of FDM molded parts[24-25]. The method is that after

the sample is formed, it is heated above the glass transition temperature (T_g), but not higher than the melting point temperature (T_m). At this time, the molecular chains inside the material gain the ability to migrate and diffuse at the interlayer boundary, and the material further crystallizes, forming a more ordered and more stable microstructure[26], releasing the internal stress generated during the molding process[27]. All of these are considered to be beneficial for the improvement of interlayer bonding performance. Yang et al.[28] controlled the crystallinity of CF/PEEK composites by regulating the ambient temperature of 3D printing and the subsequent heat treatment process, effectively enhancing the tensile strength and flexural strength. Wang et al.[29] also discovered a similar phenomenon. Wang et al.[30] achieved an improvement in the interlaminar bonding performance of fiber-reinforced PEEK composites by exploring thermal treatment methods. After continuous holding at 250 ℃ for 6 h, the interlaminar shear strength (ILSS) increased by 16%, approximately 25 MPa for CF/PEEK materials and approximately 24 MPa for GF/PEEK materials.

Adding energy input to the bonding position through an auxiliary heat source during the molding process has also been verified as an effective method. Yao et al.[31] proposed a layer-by-layer laser-assisted FDM printing process. By pre-treating the surface of the printing layer with a laser, the tensile strength of the PEEK and CF/PEEK horizontal printing components was increased by 20%, and the interlayer bonding morphology was proven to have changed through microscopic morphology. Luo et al.[32] used a laser beam to heat the deposition position, which increased the surface temperature of the sample during the extrusion molding of PEEK, strengthened the bonding degree between filaments and layers, effectively enhanced the shear strength of the sample, and achieved control over the crystallinity of the formed sample. The shear strength of the PEEK sample printed by this method increased by 45%, rising from 12.4 MPa to 17.6 MPa.

The current literature for FDM forming discontinuous fibre-reinforced PEEK composites is mainly focused on the mechanical properties of the molded samples in the horizontal direction of the enhancement effect, and the study of the mechanical properties of the interlayer is relatively small. While previous studies on processing temperature have predominantly focused on extrusion temperature and substrate temperature, the influence of chamber temperature (particularly at levels above the glass transition temperature T_g) on mechanical properties has received less attention. Therefore, further targeted investigation is necessary. Discontinuous fibers have a higher degree of freedom of molding, lighter quality, and lower raw material and manufacturing costs. However, the melt viscosity of the fiber composite material is further increased, the migration ability of the molecular chain of the high-viscosity melt in the FDM molding process will be reduced, and the material at the interface of the interlayer bonding interface is difficult to diffuse adequately even if it achieves the physical contact. For the integrated manufacturing scenario of structural circuits, the size of the formed samples is relatively large, and there are more types of forming processes. As a result, the forming equipment may not be able to set up a constant-temperature closed chamber. In addition, the heat resistance of electronic components embedded and encapsulated inside the structure during the manufacturing process is limited. They cannot withstand the high-temperature environment baking for several hours in the post-processing stage (above 200 ℃), which will lead to component damage and product failure. Therefore, it is worth conducting corresponding research on how to effectively improve the interlayer bonding performance of PEEK-based composites online. This paper focuses on discussing the performance enhancement methods of PEEK-based composites from the perspective of molding processes to improve the interlayer bonding performance of the load-bearing structure of the formed parts of structural circuit integrated manufacturing products. Firstly, the relationship between chamber temperature and horizontal tensile strength, interlayer tensile strength, and fracture type was investigated. Meanwhile, a low-cost and effective interlayer bonding performance improvement device suitable for the transformation of exist-

ing printers is proposed. By installing an auxiliary thermal radiation device on the FDM printer in its original position during the forming process, the interlayer bonding situation can be improved without the need for additional post-processing time. This can enhance manufacturing efficiency, where the heat source of the heat radiation can be absorbed by the deposited filaments, and the localised high-temperature environment created reelevates the temperature of the deposited filaments above T_g and promotes the further diffusion of the polymer chain through the interfaces of the filaments and the entanglement. At the same time, a slow-down uniform temperature is provided to the periphery to avoid warpage. To analyze the effect of this process, the influence of different output powers was studied, achieving an improvement in the interlayer bonding performance. This is conducive to further promoting the non-metallic substitution of aircraft metal structures and realizing the manufacturing and application of lightweight parts.

1 Material and Methods

1.1 Forming material and equipment

To intuitively study the effect of heat on improving interlayer bonding performance, the material used in this study was an GF/PEEK composite material (PEEK K10GF, Natural, Kexcelled, China) containing 10% by mass of chopped glass fibers, with a filament diameter of 1.75 mm, and the filaments were dried according to 110 ℃ for 6 h before moulding to avoid any possible moisture within the filaments from affecting the test results.

In this study, the used moulding equipment was a FUNMAT RPO 610HT (INTAMSYS, China) high-temperature printer. The maximum moulding size of this equipment is 600 mm × 580 mm × 580 mm, and the equipment is equipped with dual extruders with a maximum nozzle temperature of 500 ℃. The equipment has a fully enclosed moulding chamber with a maximum heating temperature of 300 ℃.

The developed thermal radiation device is shown in Fig.1. The device consists of a module and an insulation and connection module, and is installed and fixed on the extrusion module of the printer. The radiation heat source is generated by a mid-wave infrared heating tube. Mid-wave infrared radiation can cover the main absorption peaks of PEEK's carbonyl groups, ether bonds, and aromatic rings, enhancing energy absorption efficiency and enabling rapid heating of the thin layers of material deposited by FDM extrusion. The heating tube is internally gold-plated to achieve focusing, providing a uniform high-temperature environment for the current extruded material and its surroundings, thereby extending the time the extruded filament remains at its glass transition temperature. The power can be adjusted via an electronic controller to modify the intensity of thermal radiation energy. The insulation and connection modules minimize the thermal impact of the radiation heat source on non-processing areas, such as the throat, air ducts, and extrusion motor. This effectively prevents thermal disturbances to the throat cooling zone and nozzle heating sensor, ensuring smooth and balanced extrusion of the molten material from the nozzle.

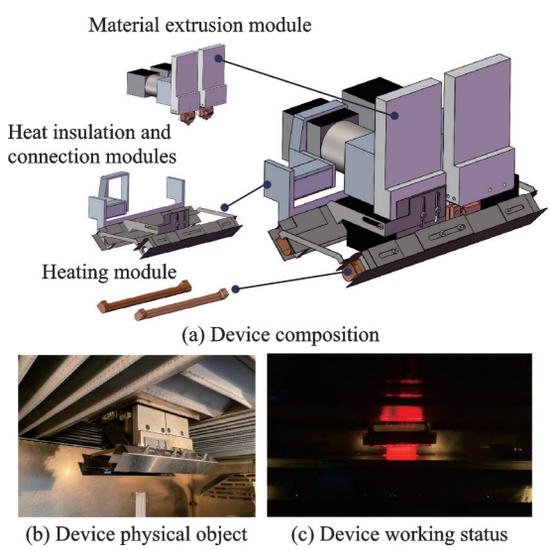

Fig.1 In situ thermal radiation device

1.2 Forming parameters and methods

All tensile specimens were prepared with identical geometry and dimensions to ensure the consistency and repeatability of the tensile tests. The specimens were modeled in STereoLithography format, and the slicing software employed was Intamsuit

4.3.0. To enhance the bonding performance of the first layer between the formed specimens and the forming substrate, a Raft auxiliary raft plate was incorporated at the bottom of each tensile specimen. Once the forming process was complete, the Raft auxiliary raft plate was detached from the tensile test specimens. The parameters shown in Table 1 were used for printing the sample parts. To meet the considerations regarding forming efficiency in actual production, the printing speed was set to 120 mm/s, which also aligns with the recommended forming speed for GF/PEEK material as specified by the equipment manufacturer. The upper limit for chamber temperature is 200 ℃, and exceeding this temperature causes the deposited material to collapse due to insufficient cooling and solidification, preventing the successful preparation of the sample parts. The remaining experimental parameters were determined based on the optimal forming parameter combinations obtained from previous research.

Table 1 Tensile sample forming parameters

Parameter	Value
Nozzle diameter/ mm	0.4
Extrusion temperature/℃	420
Layer height/mm	0.2
Printing speed (Wall)/(mm•s^{-1})	60
Printing speed (Infill)/(mm•s^{-1})	120
Chamber temperature/℃	80/110/140/170/200
Orientation	Horizontal/Vertical

In the study of interlayer bonding performance enhancement, interlayer tensile tests were conducted to evaluate the normal interlayer bonding strength of the molded parts, thereby reflecting the differences in interfacial microdefects and molecular diffusion/entanglement under different molding conditions. For this comparative validation study, a total of four groups of vertically molded samples were prepared. To eliminate the influence of other processing variables and facilitate a direct evaluation of the interlayer bonding performance, chamber heating was disabled throughout the molding process. The first group received no additional heat treatment during or after molding and served as the conventional FDM control group. The second group underwent post-process annealing at 250 ℃ with a heating/cooling rate of 10 ℃/h. The third and fourth groups were subjected to in situ thermal radiation during the molding process while chamber heating remained disabled, with heating powers of 255 W and 310 W, respectively. Based on preliminary experiments, these two heating powers were selected because heating powers below 255 W did not produce a noticeable enhancement in interlayer bonding, whereas powers above 310 W adversely affected normal sample formation.

Tensile tests were performed using standard Type 1BA specimens for molded plastics. As shown in Fig.2, the specimen preparation process is as follows: Form a tubular specimen with a triangular cross-section having a side length of 100 mm, a height of 100 mm, and a wall thickness of 3 mm. After forming, cut the specimen along the three vertices of the triangle into three flat plates. Process the flat plates using high-pressure water jet cutting to obtain the tensile specimens required for the experiment. The edges of the cut specimens are then ground and deburred using 800# waterproof sandpaper.

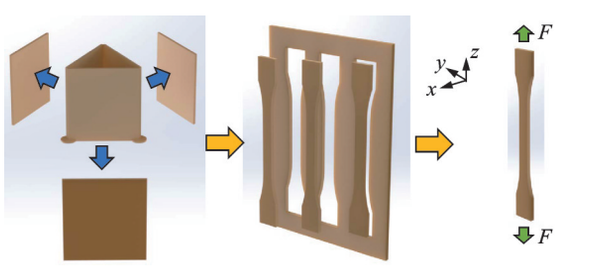

Fig.2 Preparation process of tensile specimens

1.3 Characterization and testing methods

In this study, a dynamic fatigue testing machine was employed to conduct mechanical property tests on the fabricated specimens. The testing apparatus was the LFV 100-HH (W+B Corp, Switzerland). The displacement rate during the test was set at 2 mm/min. For each parameter under investigation, five specimens were subjected to testing. The tests were carried out under an ambient temperature of 20 ℃. Subsequently, a scanning electron microscope (SEM) was utilized to observe the fracture

surface morphology of the specimens after the tensile tests. The SEM model used was Gemini SEM 300 (ZEISS, Germany). Before the SEM analysis, the specimens were sputter-coated with gold. The accelerating voltage for the SEM examination was 15 kV. Furthermore, μ-CT was utilized to measure the internal porosity of the specimens. The equipment model was FF35 (YXLON, Germany), with a minimum defect size resolution of 2 μm. The test parameters were as follows: Voltage 150 kV, current 50 μA, detector pixel size 150 μm, reconstruction ISO volume pixel side length 39.9 μm, and 1 200 projection images. The pore analysis module of VG Studio MAX 35 software was used to analyze the 3D reconstructed images obtained from CT and calculate the porosity data of the sample under different forming conditions. To eliminate the effects of noise and artifacts, pores smaller than 5 μm were filtered out during pore statistics.

Thermal property analysis was conducted using the DSC method, with relevant tests performed on the DSC3+ analyzer (Mettler-Toledo, Switzerland). Crystallinity was calculated using the equation as follows[33]

$$X_C = \frac{\Delta H_m}{(1-w)\Delta H_m^0} \times 100\%$$

where w represents the fiber content of the composite filament, ΔH_m the melting enthalpy of the composite filament, and ΔH_m^0 the theoretical melting enthalpy value of PEEK material at 100% crystallinity, with a value of 130 J/g[34].

2 Results and Discussion

2.1 Effect of chamber temperature on tensile properties

Fig.3 shows the tensile properties and Young's modulus changes of the moulded samples under different chamber temperature conditions. From the experimental results in Fig.3(a), it can be seen that for the horizontally moulded samples, the tensile strength and modulus increased significantly with the increase of chamber temperature, and the tensile strength and modulus increased from 41.11 MPa and 2.49 GPa (80 ℃ chamber temperature) to

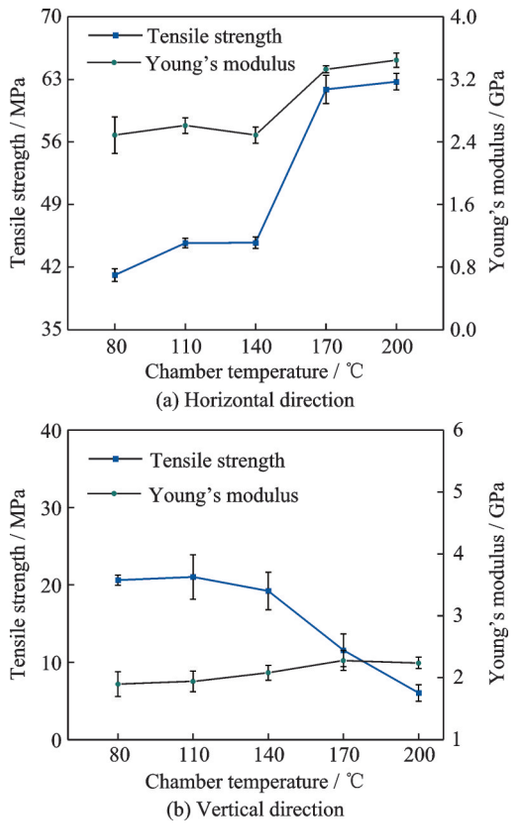

Fig.3 Variation of tensile strength and modulus with chamber temperature

62.72 MPa and 3.45 GPa (200 ℃ chamber temperature), respectively, with an increase of 52.59% and 38.58%. In the temperature range of 140—170 ℃, the mechanical properties significantly improve. This is because when forming at temperatures above the glass transition temperature of the GF/PEEK material, high cavity temperatures provide the energy and time required for polymer chains to recrystallize into continuous chains. At this point, the material can undergo isothermal crystallization, resulting in uniform crystallization and enhanced performance[24]. As can be seen from Fig.3(b), for the samples moulded vertically in the Z-direction, the tensile strength showed a tendency to be maintained smoothly, followed by a significant decrease with the increase of the chamber temperature, and the trend of modulus increased with the increase of the temperature, but with a small magnitude of change. The tensile strength and modulus changed from 20.61 MPa and 1.90 GPa (80 ℃ chamber temperature) to 6.03 MPa and 2.24 GPa (200 ℃ chamber temperature), with the changes of −70.73% and

17.94%, respectively. Increasing the chamber temperature did not increase the interlayer bonding properties in the Z-direction.

Fig.4 shows the microscopic morphology of the fracture section of the horizontally formed sample at the position where the key tensile data changes. Figs.4(a) and (b) respectively present the morphologies when the chamber temperature is 80 ℃ and 110 ℃. The contact area between the deposited filaments in the horizontal layer is insufficient, and there are significant pore defects. The contact parts between the deposited filaments in adjacent layers undergo local deformation due to mutual mechanical interference, and no large-area fusion interface was formed. The fracture surface presents typical plastic deformation characteristics. As the temperature increases, as shown in Fig.4(c), when the chamber temperature reaches 200 ℃, the boundaries between the transversely deposited filaments completely disappear, while the interlayer interfaces between the longitudinal layers remain intact, but their bonding area significantly increases compared to the 80 ℃ condition. The contact area between the deposited filaments within the same forming layer increases, leading to enhanced penetration and diffusion between the filaments, thereby improving mechanical properties[35].

Fig.5 shows the cross-sectional morphology of the vertically formed part. At a chamber temperature of 80 ℃, the boundaries of the deposited filaments inside the specimen are clearly defined, and the cross-section exhibits a mixed failure mode characterized by extensive interlaminar separation failure and partial internal fracture failure of the deposited filaments. Interlaminar separation failure refers to the neat separation of the upper and lower layers of deposited filaments along their contact interface. Fractures within the deposited filaments occur at the corners of the filling trajectory. At the fracture locations at the corners, distinct fiber pull-out features are observed, which only appear when fractures occur within the deposited filaments. When the chamber temperature was increased to 110 ℃, the boundaries between horizontal filaments inside the specimen began to transition from distinct to blurred compared to 80 ℃, with further signs of fusion. The cross-section exhibited a mixed failure mode of interlaminar separation and internal fractures within the deposited filaments. However, the cross-section now exhibits numerous holes and grooves left by pulled fibers, and the fracture surface morphology

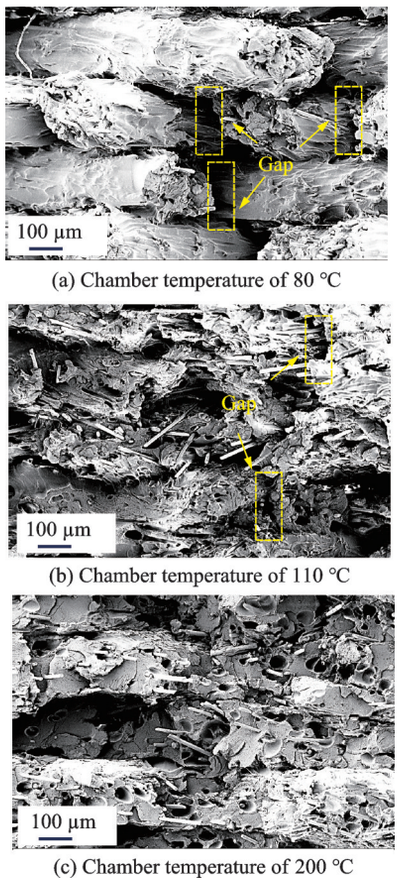

Fig.4 Fracture section morphologies of the horizontally formed sample

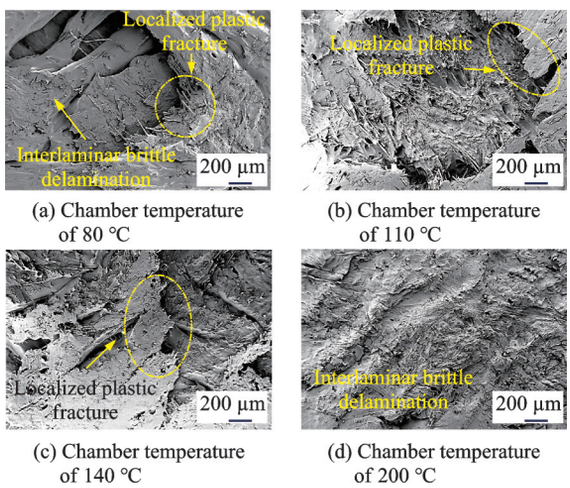

Fig.5 Fracture section morphologies of the vertical forming sample

becomes rougher. The proportion of internal fiber breakage failure increases, indicating that the elevated chamber temperature enhances the bonding between materials. At a chamber temperature of 140 ℃, the fracture failure forms inside the specimen are similar to those at 110 ℃, but the fracture locations exhibit smooth morphological characteristics, with only a small amount of fiber pull-out observed. This indicates a decrease in bonding performance, with fracture locations tending toward the contact interface between the upper and lower layers of deposited fibers. At a chamber temperature of 200 ℃, the cross-section exhibits a single interlayer separation failure mode, with a few fibers pulled out during interlayer fracture. The interfaces between deposition threads within the same layer are not prominent, and the bonding is good, but the bonding strength at the interlayer interfaces is weak, potentially serving as the initiation point for cracks during failure. As shown in Fig.6, the ineffective improvement in interlayer bonding performance is likely due to the longer printing interval between layers compared to the time between filaments within the same layer. In a prolonged high-temperature environment, the crystallization time of the deposited layer material increases, resulting in larger crystal sizes and higher crystallinity. The proportion of amorphous regions between layers is small, and numerous crystals are arranged near the side of the already deposited layer on the interlayer contact surface. The molecular chains of the current printed layer can only diffuse near the contact surface and cannot penetrate the crystals, resulting in a reduced density of molecular chain links between layers, which negatively impacts interlayer bonding strength[36]. Conversely, when the chamber temperature is within an appropriate range, the crystal size and density within the deposited layer decrease, allowing molecular chains between layers to have more space and opportunities for mutual diffusion and cross-linking, thereby enhancing interlayer bonding performance. The crystallinity of the fracture location of the test specimen under different chamber temperature conditions is compared in Table 2. As the chamber temperature increases, the

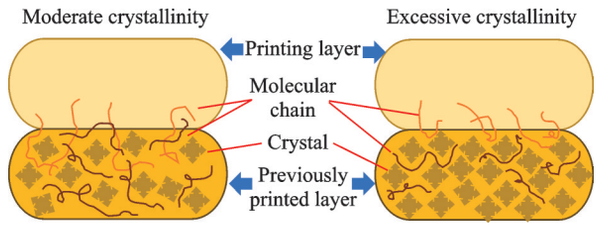

Fig.6 Molecular chain diffusion and cross-linking under different crystallisation conditions

degree of crystallinity gradually increases, reaching a maximum of 28.53% at a chamber temperature of 170 ℃.

Table 2 Crystallinity of moulded parts formed at different chamber temperatures

Chamber temperature/℃	Degree of crystallisation/%
80	13.37
110	19.05
140	22.04
170	28.53
200	27.37

2.2 Experiments and analyses for improving interlayer bonding performance

In order to enhance the interlayer bonding performance, samples were moulded using the in situ thermal radiation device designed in this study. Since the IR energy is mainly absorbed by the material surface, its local and rapid heating effect can locally remelt the surface of the previously deposited layer before the new layer is extruded to provide sufficient energy at the bonding interface, and promote optimal molecular diffusion and bonding without leading to over-crystallisation or degradation of the host material. The surface morphology and surface roughness of the outer wall of the moulded samples under different conditions are shown in Fig.7. Fig.7(a) shows the surface morphology of the samples under four different conditions, namely, standard FDM moulding, annealing treatment after standard FDM moulding, the use of in situ thermal radiation during the moulding process (255 W power), and the use of in situ thermal radiation during the moulding process (310 W power). Fig.7(b) shows the surface roughness testing results, and Fig.7(c) shows the surface melting and collapsing morphology after the

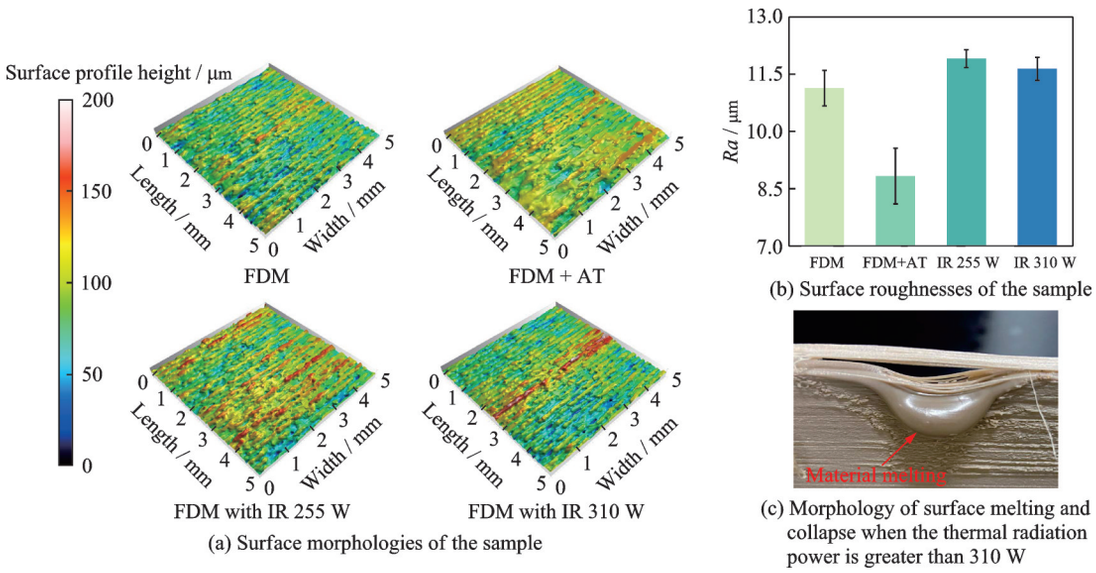

Fig.7 Comparison of surface morphology and roughness of the sample

thermal radiation power is higher than 310 W. Comparing Fig.7(a), it can be found that the corrugated features of the FDM process can be observed in all four morphologies, with the difference that the interlayer fusion phenomenon appears in some areas of the sample surfaces other than the standard FDM moulding conditions, which is the most obvious phenomenon in annealed samples. For the surface roughness results in Fig.7(b), the heat-treated sample showed the lowest *Ra* value of 8.83 μm, while the *Ra* values for the in situ thermal radiation moulded samples were similar to those of the standard moulding process, ranging from 11 μm to 12 μm. This indicates that, within the current allowable thermal radiation power range, in situ thermal radiation does not significantly improve surface morphology, but it also does not have any adverse effects. Whereas when the power is too high (320 W), the collapse phenomenon as shown in Fig.7(c) occurs, resulting in the samples not being able to be formed properly.

A comparison of the *Z*-axis tensile properties of the moulded samples under different moulding conditions is shown in Fig.8. Compared with the standard FDM moulded samples, the tensile properties and strain-at-break rates of the samples that were annealed and heat-treated after moulding, as well as the samples that were moulded using in situ thermal radiation-assisted moulding, were enhanced. The maximum tensile strength of 27.54 MPa was achieved under in situ thermal radiation-assisted forming conditions at a power parameter of 255 W. Compared to the maximum tensile strength of 24.70 MPa obtained after annealing heat treatment, this represents an increase of 26.54%.

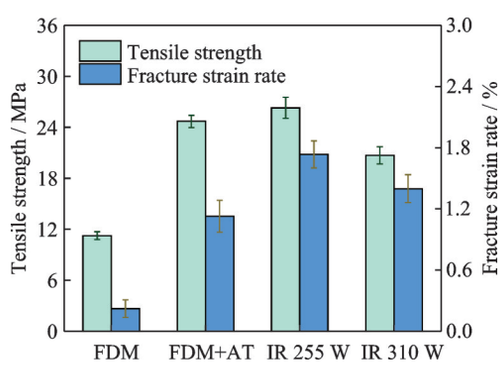

Fig.8 Performance comparison among different molding conditions

Compared to the tensile strength of 11.25 MPa achieved using FDM forming alone, this represents an increase of 2.34 times by using in situ thermal radiation. Compared to the tensile strength in the horizontal direction, the vertical tensile strength under the 255 W thermal-assisted forming conditions reached 43.91% of the horizontal tensile strength (formed at 200 ℃ chamber temperature) and peaked at 66.99% of the horizontal tensile strength (formed at 80 ℃ chamber temperature). In the study of fracture ductility, the highest values were obtained under 255 W in situ thermal radiation

(1.74%), followed by 310 W in situ thermal radiation (1.40%), and heat-treated samples (1.12%), while the standard FDM moulding had a fracture ductility of only 0.22%. Compared with standard FDM moulding, the fracture ductility using in situ thermal radiation moulding is 7.91 times higher than that of standard FDM moulding. Based on the changes in the above data, the in situ thermal radiation-assisted moulding can improve the bonding strength and fracture toughness between layers in the vertical direction of the sample.

To study the bonding behavior of the interlayer interface under the action of in situ thermal radiation, the cross-section morphology of the samples was observed using an optical microscope as shown in Fig.9. Fig.9(a) shows a standard FDM moulding sample. With a neat cross-section, cracks expand along the straight line of the interlayer contact location, smooth fracture surface, and the fracture form of brittle fracture and segregation of the interlayer bonding interface. Fig.9(b) shows the sample with annealing treatment after moulding. The section is generally neat, and the cracks are deflected in some regions, showing a mixed mode of interlayer fracture and intralayer fracture. Fig.9(c) shows the 255 W in situ thermal radiation moulding sample, where the cross-section no longer follows a regular straight line. The cracks deflect several times during propagation, and the interface exhibits distinct internal fracture behavior within the deposition filaments, indicating that some of the interlayer interfaces are stronger than the internal bonding strength of the filaments. Fig.9(d) shows the 310 W in situ thermo-radiation moulding samples. The sectional morphology exhibits similar characteristics to those in Fig.9(b), but the number of adherent debris in the fractured material is slightly higher, which is thought to be the reason why the tensile strength data of the 310 W in situ thermo-radiation moulding samples are lower than those of the heat-treated samples but the ductility of them appears to be increased.

Further analysis using SEM of the fracture locations and cross-sections of molded specimens under different conditions revealed significant differences in the failure characteristics between the fibers and the PEEK matrix across specimens formed under varying conditions. Fig.10(a) shows a standard FDM-formed specimen, where the primary fracture mode is interfacial brittle delamination, with small areas of ductile plastic fracture observed at the contact points between filaments[37]. These locations are presumed to have formed due to compression by the nozzle and contact with the nozzle's outer wall during material extrusion. No obvious fiber pull-out phenomena were observed across the entire cross-section, indicating that no fiber-PEEK interface separation occurred during fracture. Fig.10(b) shows the cross-section of the post-annealed specimen, where the smooth surface of the deposited filaments remains visible, but the proportion of ductile plastic fracture regions has increased. This is clearly due to the annealing process providing conditions for re-bonding between the deposited filaments[1]. The degree of plastic deformation in the fracture increased, and there were more distinct fracture separation features along the fiber-PEEK matrix interface. Fig.10(c) shows a specimen formed by in situ thermal radiation at 255 W, where the smooth interlayer interface has been replaced by irregular fracture morphology. The fractures primarily occur within the deposited filaments, with a large number of ex-

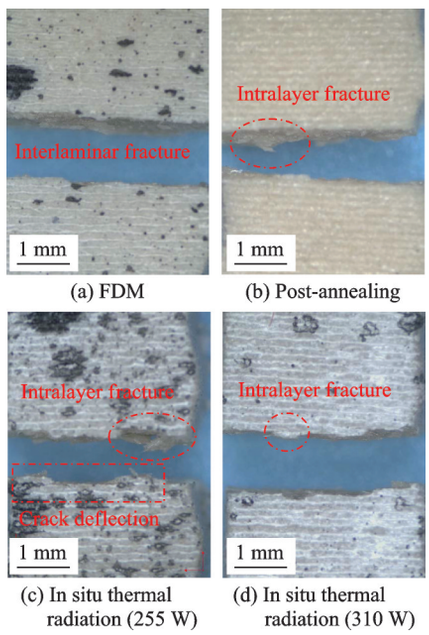

Fig.9 Cross-sectional morphologies under different forming conditions

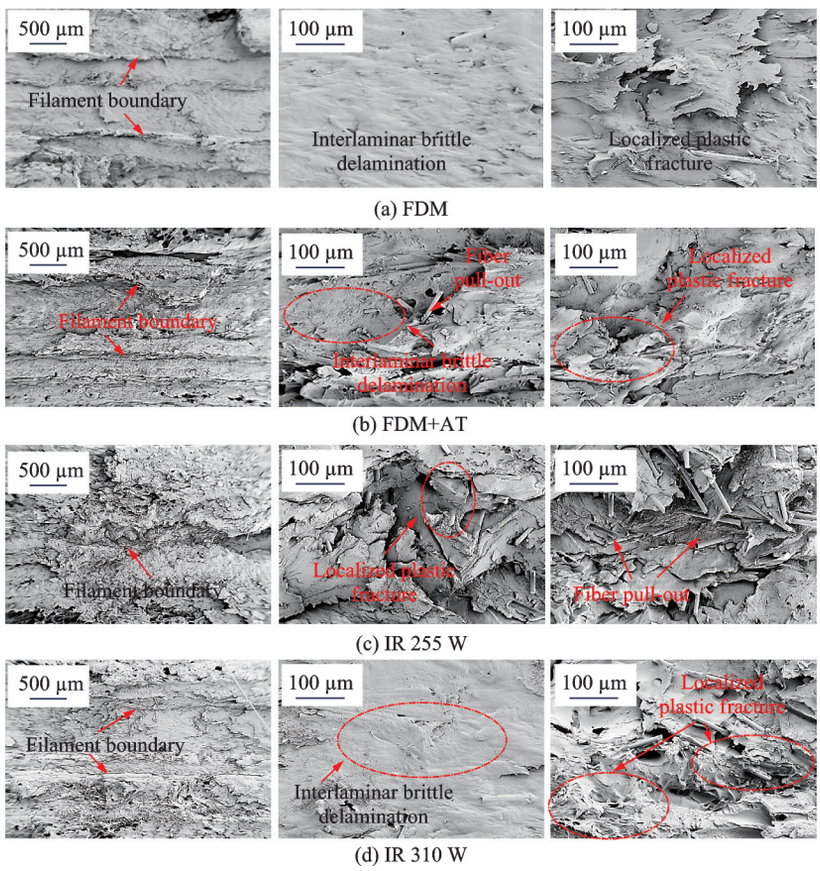

Fig.10 Comparison of the fracture cross-sectional morphologies of tensile samples under different forming conditions

posed glass fibers at the fracture sites. The thinnest position in the vertical direction of the formed part has shifted from the interlayer deposition filament contact interface to the interface between the fibers and the PEEK matrix, specifically at the weaker interface between the fibers within the deposition filament and the PEEK material. Fig.10(d) shows the in situ thermal radiation-formed sample at 310 W. Its cross-sectional features are similar to those in Fig.10(b), still a mixture of smooth filament interfaces and local plastic deformation failure features.

Fig.11 shows the comparison of the pore distribution inside the standard FDM process-formed sample obtained by CT scanning and the sample formed using in situ thermal radiation (power 255 W). Both samples have pore defects inside, but the pore size and content of the standard FDM process-formed sample are higher than those of the in situ thermal radiation-formed sample. According to the test results of the CT analysis software, the porosity of the standard FDM process-formed sample is 5.26%, and that of the in situ thermal radiation-

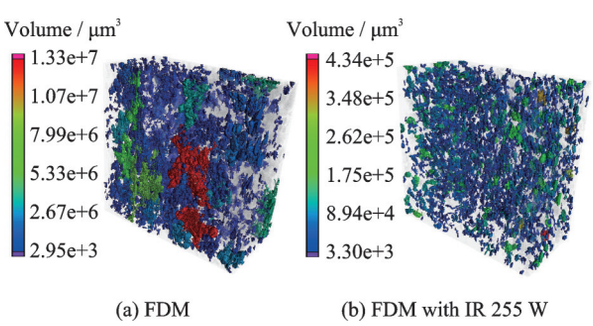

Fig.11 Comparison of the internal pore morphologies of directly formed samples and thermal radiation-formed samples

formed sample is 2.95%. The porosity of the in situ thermal radiation-formed sample is significantly lower than that of the standard FDM process-formed sample. Comparing the morphology of the pores, the standard FDM process formed sample has large, continuous sheet-like pores inside, which are caused by the poor interlayer bonding and the gaps between the deposited filaments. The rest of the smaller pores are from the interior of the composite material[28]. The in situ thermal radiation-formed sample has smaller pore sizes inside, mainly com-

posed of the gaps between filaments within the same layer and the interior of the composite material. The porosity within the material is also a factor affecting interlayer bonding performance. Within the same volume, the more pores there are, the smaller the contact area between the deposited filaments, resulting in a reduced effective load-bearing area when subjected to external forces, thereby decreasing the material's load-bearing capacity[38]. Additionally, pore locations are more prone to stress concentration, making them susceptible to becoming crack initiation points under load, leading to premature failure in the vertical direction[23].

In conclusion, analysis of the fracture morphology and internal pore distribution reveals that the sample formed using 255 W in situ thermal radiation exhibits more compact internal bonding. During the forming process, the thermal radiation device delivers directional energy to the deposited layer, raising the interlayer interface temperature close to the melting point. This localized thermal environment enhances the wetting, flow, and diffusion of the PEEK matrix at the composite material's interlayers. The flow of PEEK also improves the fiber-matrix interface, reducing internal pore defects[39]. At the same time, it also helps to release stress and improve the dimensional stability of the formed parts[40]. The rougher cross-sectional morphology also proves that the degree of intermolecular diffusion at the bonding interface is greater, the degree of mutual wetting between interfaces increases, and the stress acting on the interlayer bonding interface can be uniformly released[41].

3 Conclusions

The effects of different chamber temperatures on the tensile properties and micro-morphology of GF/PEEK composites were investigated by experimental methods. An in situ thermal radiation device was developed to enhance the interlayer bonding properties in the *Z*-direction. Furthermore, the effects of thermal radiation on surface morphology, surface roughness, interlayer bonding strength, and microstructural characteristics of the fabricated specimens were examined. The conclusions are as follows:

(1) The chamber temperature has an impact on the tensile properties and modulus of PEEK-based composite materials. Increasing the chamber temperature can enhance the tensile properties and modulus of the horizontally printed samples. The increase in chamber temperature can increase the modulus of the vertically printed samples, but it cannot effectively enhance the interlayer tensile strength.

(2) The designed in situ thermal radiation device can significantly enhance the strength of the interlayer bonding interface of the sample without damaging the surface morphology, while also increasing the fracture ductility of the sample. Compared with the standard FDM formed sample, the tensile properties have increased by 2.34 times, and the fracture ductility has increased by 7.91 times.

(3) Cross-sectional microstructural analysis confirms that the performance enhancement is attributed to the increased interfacial density and the enhanced interdiffusion of polymer chains across adjacent layers induced by thermal radiation. Moreover, the fracture form of the interface after strengthening changes from the original fracture along the interface between fibers to a mixed form of fracture at the interface between fibers and within the fibers.

References

[1] LI W H, HUANG W Z, XIONG Y, et al. Failure mechanism and heat treatment effect of 3D-printed bio-inspired helicoidal CF/PEEK composites[J]. Composites Communications, 2023, 37: 101464.

[2] NGO T D, KASHANI A, IMBALZANO G, et al. Additive manufacturing (3D printing): A review of materials, methods, applications and challenges[J]. Composites Part B: Engineering, 2018, 143: 172-196.

[3] BERRETTA S, DAVIES R, SHYNG Y T, et al. Fused deposition modelling of high temperature polymers: Exploring CNT PEEK composites[J]. Polymer Testing, 2017, 63: 251-262.

[4] HUANG Zedong, WANG Kun, CAI Deng'an, et al. Fibre distribution and tensile properties of composite grid structure stiffeners[J]. Journal of Nanjing University of Aeronautics & Astronautics, 2024, 56(3): 478-485. (in Chinese)

[5] ZHAO Y C, ZHAO K, LI Y C, et al. Mechanical

characterization of biocompatible PEEK by FDM[J]. Journal of Manufacturing Processes, 2020, 56: 28-42.

[6] CHEN P, WANG H Z, SU J, et al. Recent advances on high-performance polyaryletherketone materials for additive manufacturing[J]. Advanced Materials, 2022, 34(52): 2200750.

[7] LI N, CHEN J L, LIU H S, et al. Effect of preheat treatment on carbon fiber surface properties and fiber/PEEK interfacial behavior[J]. Polymer Composites, 2019, 40(S2): E1407-E1415.

[8] MACDONALD E, WICKER R. Multiprocess 3D printing for increasing component functionality[J]. Science, 2016, 353(6307): aaf2093.

[9] CHACÓN J M, CAMINERO M A, GARCÍA-PLAZA E, et al. Additive manufacturing of PLA structures using fused deposition modelling: Effect of process parameters on mechanical properties and their optimal selection[J]. Materials & Design, 2017, 124: 143-157.

[10] RINALDI M, GHIDINI T, CECCHINI F, et al. Additive layer manufacturing of poly (ether ether ketone) via FDM[J]. Composites Part B: Engineering, 2018, 145: 162-172.

[11] ARIF M F, KUMAR S, VARADARAJAN K M, et al. Performance of biocompatible PEEK processed by fused deposition additive manufacturing[J]. Materials & Design, 2018, 146: 249-259.

[12] ZANJANIJAM A R, MAJOR I, LYONS J G, et al. Fused filament fabrication of PEEK: A review of process-structure-property relationships[J]. Polymers, 2020, 12(8): 1665.

[13] ZHANG Q, SHI Y, GAO C F. Research progress of multicomponent and multilevel 3D printing materials [J]. Transactions of Nanjing University of Aeronautics & Astronautics, 2024, 41(1): 1-34.

[14] LI Yong, ZHU Kang, LIU Hongquan, et al. Review of in situ polymerization of thermoplastic composites and its forming process[J]. Journal of Nanjing University of Aeronautics & Astronautics, 2023, 55(1): 1-11. (in Chinese)

[15] GAO S S, LIU R J, XIN H, et al. The surface characteristics, microstructure and mechanical properties of peek printed by fused deposition modeling with different raster angles[J]. Polymers, 2022, 14(1): 77.

[16] WANG P, ZOU B, DING S L, et al. Effects of FDM-3D printing parameters on mechanical properties and microstructure of CF/PEEK and GF/PEEK[J]. Chinese Journal of Aeronautics, 2021, 34(9): 236-246.

[17] YIN J, LU C H, FU J Z, et al. Interfacial bonding during multi-material fused deposition modeling (FDM) process due to inter-molecular diffusion[J]. Materials & Design, 2018, 150: 104-112.

[18] WANG P, ZOU B, XIAO H C, et al. Effects of printing parameters of fused deposition modeling on mechanical properties, surface quality, and microstructure of PEEK[J]. Journal of Materials Processing Technology, 2019, 271: 62-74.

[19] CURMI A, ROCHMAN A, BUHAGIAR J. Influence of polyetheretherketone (PEEK) viscosity on interlayer shear strength in screw extrusion additive manufacturing[J]. Additive Manufacturing, 2024, 84: 104086.

[20] ZHOU H, CHENG X, JIANG X L, et al. Study of the interlayer bonding strength for combined 3D printing and milling of polyetheretherketone[J]. Journal of Applied Polymer Science, 2023, 140(17): e53773.

[21] ABBAS K, HEDWIG L, BALC N, et al. Advanced FFF of PEEK: Infill strategies and material characteristics for rapid tooling[J]. Polymers, 2023, 15(21): 4293.

[22] VAEZI M, YANG S. Extrusion-based additive manufacturing of PEEK for biomedical applications[J]. Virtual and Physical Prototyping, 2015, 10(3): 123-135.

[23] YANG K Y, SHAN Z D, CHEN Y W, et al. Research on the optimization of *Z*-direction forming process for additively manufactured polyetheretherketone composite in environments without bed and chamber heating[J]. Polymer Composites, 2025, 46(17): 15909-15923.

[24] YANG C C, TIAN X Y, LI D C, et al. Influence of thermal processing conditions in 3D printing on the crystallinity and mechanical properties of PEEK material[J]. Journal of Materials Processing Technology, 2017, 248: 1-7.

[25] BHANDARI S, LOPEZ-ANIDO R, GARDNER D. Enhancing the interlayer tensile strength of 3D printed short carbon fiber reinforced PETG and PLA composites via annealing[J]. Additive Manufacturing, 2019, 30: 100922.

[26] ZHEN H L, BIN Z, LONG Q, et al. Effect of 3D printing process parameters and heat treatment conditions on the mechanical properties and microstructure of peek parts[J]. Polymers, 2023, 15(9): 2209.

[27] HAN X T, DONG Y, YANG C C, et al. Carbon fiber reinforced PEEK composites based on 3D-printing technology for orthopedic and dental applications[J]. Journal of Clinical Medicine, 2019, 8(2): 240.

[28] YANG D, CAO Y, ZHANG Z K, et al. Effects of crystallinity control on mechanical properties of 3D-

printed short-carbon-fiber-reinforced polyether ether ketone composites[J]. Polymer Testing, 2021, 97: 107149.

[29] WANG Z G, ZHANG B Y, LI Y X. Mechanical characterization of PEEK-CF/PEEK sandwich structures prepared via a combination of fused filament fabrication and epoxy post-bonding[J]. Journal of Adhesion Science and Technology, 2024, 38(17): 3290-3315.

[30] WANG P, ZOU B. Improvement of heat treatment process on mechanical properties of FDM 3D-printed short-and continuous-fiber-reinforced PEEK composites[J]. Coatings, 2022, 12(6): 827.

[31] YAO J M, DUONGTHIPTHEWA A, XU X G, et al. Interlayer bonding improvement of PEEK and CF-PEEK composites with laser-assisted fused deposition modeling[J]. Composites Communications, 2024, 45: 101819.

[32] LUO M, TIAN X Y, ZHU W J, et al. Controllable interlayer shear strength and crystallinity of PEEK components by laser-assisted material extrusion[J]. Journal of Materials Research and Technology, 2018, 33(11): 1632-1641.

[33] KE Yangchuan, ZHENG Yubin, WU Zhongwen. The measurements of crystallinity degree of PEEK [J]. Chinese Journal of Materials Research, 1996, 10 (2): 205-209.(in Chinese)

[34] BLUNDELL D J, OSBORN B N. The morphology of poly (aryl-ether-ether-ketone)[J]. Polymer, 1983, 24(8): 953-958.

[35] NAGANABOYINA H P S, NAGARAJU P, SONAYE S Y, et al. In-house processing of carbon fiber-reinforced polyetheretherketone (CFR-PEEK) 3D printable filaments and fused filament fabrication-3D printing of CFR-PEEK parts[J]. The International Journal of Advanced Manufacturing Technology, 2023, 128(11): 5011-5024.

[36] VAES D, COPPENS M, GODERIS B, et al. The extent of interlayer bond strength during fused filament fabrication of nylon copolymers: An interplay between thermal history and crystalline morphology[J]. Polymers, 2021, 13(16): 2677.

[37] BAILEY R, BADER M. Fibre pull-out phenomena in reinforced polyamides[J]. Journal of Materials Science Letters, 1985, 4: 843-844.

[38] FU Y T, LI J, GUO F L, et al. Micro-structure and tensile property analyses of 3D printed short carbon fiber reinforced PEEK composites[J]. Composites Communications, 2023, 41: 101655.

[39] FAN Congze, SHAN Zhongde, ZOU Guisheng, et al. Performance of short fiber interlayered reinforcement thermoplastic resin in additive manufacturing[J]. Materials, 2020, 13(12): 2868.

[40] SUN Q L, SHAN Z D, ZHAN L H, et al. Warp deformation model of polyetheretherketone composites reinforced with carbon fibers in additive manufacturing[J]. Materials Research Express, 2021, 8(12): 125305.

[41] ZHANG X, WANG J L. Controllable interfacial adhesion behaviors of polymer-on-polymer surfaces during fused deposition modeling 3D printing process[J]. Chemical Physics Letters, 2020, 739: 136959.

Acknowledgement This work was supported by the National Key Research and Development Program of China (No.2023YFB4603900).

Authors

The first author Mr. **LI Haozhen** received the M.S. degree from Qingdao University of Technology, Qingdao, China, in 2017. He is currently pursuing a Ph.D. degree at College of Mechanical Engineering, Nanjing University of Science and Technology. His research focuses on the additive manufacturing of polymer composites and structural electronics.

The corresponding authors Dr. XIAO Xingzhi received his Ph.D. degree from Nanjing University of Science and Technology, Nanjing, China, in 2018. He is currently an associate professor at Nanjing University of Science and Technology. His research focuses on multi-material additive manufacturing. Prof. **LIAO Wenhe** received his M.S. and Ph.D. degrees from Nanjing University of Aeronautics and Astronautics, Nanjing, China, in 1990 and 1996, respectively. He is a professor at Nanjing University of Science and Technology. His research focuses on additive manufacturing and the design and manufacturing of micro/nano satellites.

Author contributions Mr. **LI Haozhen** designed the study, carried out machining tests, interpreted the results, and wrote the manuscript. Dr. **XIAO Xingzhi** optimized the overall idea and feasibility of the proposed method. Prof. **LIAO Wenhe** guided the research and assisted in manuscript revisions. Prof. **LIU Tingting** contributed to the review and structure refinement of the manuscript. All authors commented on the manuscript draft and approved the submission.

Competing interests The authors declare no competing interests.

(Production Editor: SUN Jing)

优化热输入提升玻纤强化聚醚醚酮增材制造层间结合

李昊真，肖行志，廖文和，刘婷婷

（南京理工大学机械工程学院，南京 210094，中国）

摘要：针对大型玻璃纤维强化聚醚醚酮（Glass fiber-reinforced polyetheretherketone，GF/PEEK）复合材料构件及结构电路一体化制造构件成形后难以实施整体热处理、导致熔融沉积成形（Fused deposition modeling，FDM）构件层间结合性能不足的问题，提出一种适用于成形过程的原位热辐射强化方法，以提升构建方向的层间力学性能。通过调控成形腔室温度和原位热辐射功率，结合拉伸试验、层间拉伸试验及断口微观形貌分析，对不同热处理方式下GF/PEEK复合材料的力学性能及层间强化机制进行了研究。结果表明：提高腔室温度能够改善水平方向力学性能，当腔室温度为200 ℃时，样件拉伸强度和杨氏模量分别达到62.72 MPa和3.45 GPa；但层间拉伸强度由20.61 MPa降低至6.03 MPa，而层间杨氏模量由1.90 GPa提高至2.24 GPa。采用原位热辐射强化后，构建方向样件的层间结合性能显著提升，当热辐射功率为255 W时，垂直拉伸强度和断裂延展性分别提高至普通FDM样件的2.34倍和7.91倍，其性能接近成形后热处理样件。断口形貌分析表明，原位热辐射促进了层间聚合物分子扩散与缠结，减少了界面孔隙等缺陷，从而显著增强了层间结合性能。该方法无需增加成形后整体热处理工序即可有效提升GF/PEEK复合材料FDM构件的层间力学性能，为高性能热塑性复合材料复杂构件的增材制造提供了有效的工艺途径。

关键词：聚醚醚酮；增材制造；层间结合强度；复合材料；热辐射

研究亮点：

1. 提出了一种适用于GF/PEEK复合材料熔融沉积成形过程的原位热辐射强化方法，无需成形后整体热处理即可提高层间结合性能。

2. 揭示了成形腔室温度与原位热辐射对GF/PEEK复合材料力学性能的不同作用规律，并在本研究工艺条件下确定了255 W为最佳原位热辐射功率。

3. 阐明了原位热辐射通过促进层间聚合物分子扩散与缠结、减少界面缺陷实现层间强化的作用机制。